MULTISCALE AM-FM ANALYSIS OF PNEUMOCONIOSIS X-RAY IMAGES

Victor Murray[†,♮], *Marios S. Pattichis*[†], *Herbert Davis*[♮], *Eduardo S. Barriga*[†,♮] *and Peter Soliz*[♮]

[†]University of New Mexico, Department of Elect. and Comp. Eng., Albuquerque, New Mexico, U.S.A.
[♮]VisionQuest Biomedical, Albuquerque, New Mexico, U.S.A.
E-mails: vmurray@ieee.org, pattichis@ece.unm.edu, {bert,sbarriga,psoliz}@visionquest-bio.com

ABSTRACT

This paper presents a computer-aided diagnostic (CAD) system for analyzing chest radiographs based on the International Labor Organization (ILO) standards. We introduce an amplitude-modulation frequency-modulation (AM-FM) based methodology by which a computer-based system will extract AM-FM features and detect those with suspected interstitial lung diseases. For classification, we use Partial Least Squares (PLS) using a low number of extracted factors (making the system robust). We consider several different AM-FM classifiers based on extracting features from individual scales as well as a final classifier that combines results from the individuals scales. We validate our methodology on 11 standard images graded according to the ILO standard. For several scales, as well as for the combined classifier that uses information from all scales, we get excellent classification results (area under the receiver operator characteristics curve equal to 1.0) using a limited number of latent PLS factors.

Index Terms— AM-FM, X-ray chest imaging

1. INTRODUCTION

Millions of workers worldwide, including the United States, are exposed to inorganic dusts that may lead to occupational lung disease. The chest radiograph is an essential tool used in the screening, surveillance, and diagnosis of dust-related respiratory illness resulting from silica and coal dust, asbestos, and a variety of other dusts that can lead to disease. The standardized method used by the International Labor Organization (ILO, [1]) for interpreting the chest radiograph for inorganic dust-induced diseases or pneumoconioses has been widely utilized for the past five decades.

Two limitations of the current ILO system are the intra- and inter-interpreter variability and the time consuming process of interpreting large numbers of radiographs taken for screening and surveillance programs. Today, there is a rapid transition from film media to digital radiology. Automation will play a significant role in the solution to growing health care costs, and most importantly, smooth the transition to digital by providing a link between visual interpretation of the film images to analysis of digital chest radiographs. The CAD system described in this paper is intended to provide a reliable, sensitive, and cost-effective method of screening chest radiographs for pneumoconiosis and significantly decrease the time required by readers trained in the ILO method to review large numbers of radiographs from preventative programs for workers exposed to inorganic dusts.

In 2001, Van Ginneken et al. presented a survey for computer-aided diagnosis in chest radiographs including texture analysis in the detection of pneumoconiosis, or coal miners disease [2]. Prior work in this area of detection of pneumoconiosis includes the use of binarized images with Neural Networks to detect opacities [3, 4]. In [5], we used logic functions to analyze pneumoconiosis image symmetries, inter-reader variability, and disease progression from the human classification of chest radiographs. In prior work, we investigated the use of spatial gray level dependence matrices (SGLDM) and gray level difference statistics (GLDS) with different classifiers for classifying different regions of interest [6].

In this paper, we consider a new multi-scale approach based on Amplitude-Modulation Frequency-Modulation (AM-FM) methods [7, 8]. Images are analyzed over a dyadic filter-bank and AM-FM image features are extracted from different scales. For each pixel, we obtain dominant instantaneous frequency (IF) and instantaneous amplitude (IA) estimates. Here, we hypothesize that objects such as ribs, blood vessels, opacities and other structures will be represented by different characteristic IF and IA features that can be successfully extracted and used in subsequent image classification. The system uses different scales and scale combinations to capture the widely varying frequencies that may be present. We use Partial Least Squares (PLS) to perform the classification using a very limited number of factors (making the system robust).

We summarize the methodology in section 2. Results are given in section 3 and a discussion is given in section 4. We have concluding remarks in section 5.

2. METHODOLOGY

2.1. Database Used

The database used for these results was obtained from chest radiographs taken from miners from the Miners' Colfax Medical Center and the Grant's Uranium Miners, Raton, New Mexico. We use 11 X-Rays images from different patients graded according to the ILO standard for profusion of opacities: (i) 4 patients in category 0/0, (ii) 4 patients in category 1/1 and (iii) 3 patients in category 2/2, where 0/0 implies no signs of opacities and progressively more opacity profusion is graded from 1/1 to 2/2. Each X-Ray image is 4200x5100 pixels and digitalized in uncompressed TIF format at 300 dpi resolution. We performed a rough, manual segmentation using rectangular ROI regions of the right and left lungs, producing a total of 22 input images. Each segmented region was 1600x1400 pixels per lung and covered the upper region of the lung as shown in Fig. 1.

To improve the contrast of the digitalized X-Rays, we applied a logarithmic transformation to the images [9]. For each input image $I(\cdot)$, we produce an image $I_n(\cdot)$ such that $I_n(\cdot) = \log_{10}(1 + 10^n I(\cdot))$. For our database, we used the fixed value of $n = -2$ to improve the visual display of the images (see [9] for details).

2.2. AM-FM Methods

We consider multi-scale AM-FM representation of digital non-stationary images given by [8, 10, 11]

$$I(k_1,k_2) \approx \sum_{n=1}^{M} a_n(k_1,k_2)\cos\varphi_n(k_1,k_2), \quad (1)$$

where $n = 1,2,\ldots,M$ denote different scales, $a_n(k_1,k_2)$ denotes slowly-varying instantaneous amplitude (IA) function and $\varphi_n(k_1,k_2)$ denotes the instantaneous phase (IP) functions. The basic idea is to let the frequency-modulated (FM) components $\cos\varphi_n(k_1,k_2)$ capture fast-changing spatial variability in the image intensity. The instantaneous frequency (IF) $\nabla\varphi_n(k_1,k_2)$ is defined in terms of the gradient of the IP: $\nabla\varphi_n(k_1,k_2) = (\partial\varphi_n/\partial k_1(k_1,k_2),\ \partial\varphi_n/\partial k_2(k_1,k_2))$.

For a single-scale AM-FM representation ($M = 1$ in (1)), the IA and the IP are estimated using [12] $\hat{a}(k_1,k_2) = |\hat{I}_{AS}(k_1,k_2)|$ and $\hat{\varphi}(k_1,k_2) = \arctan\left(\text{imag}(\hat{I}_{AS}(k_1,k_2))/\,\text{real}(\hat{I}_{AS}(k_1,k_2))\right)$, respectively, with $\hat{I}_{AS}(k_1,k_2) = I(k_1,k_2) + j\mathcal{H}_{2d}[I(k_1,k_2)]$, where $\mathcal{H}_{2d}$ denotes a two-dimensional extension of the one-dimensional Hilbert transform operator. For robust IA and IF estimations, we use a variable spacing, local linear phase (VS-LLP) method as described in [8, 10]. Here, for estimating the first component, we generate four estimates using:

$$\hat{\varphi_1}(k_1,k_2) = \frac{1}{n_1}\arccos\left(\frac{\bar{I}_{AS}(k_1+n_1,k_2)+\bar{I}_{AS}(k_1-n_1,k_2)}{2\bar{I}_{AS}(k_1,k_2)}\right), \quad (2)$$

where $\bar{I}_{AS}(k_1,k_2) = \hat{I}_{AS}(k_1,k_2)/|\hat{I}_{AS}(k_1,k_2)|$, n_1 represents a variable displacement, from 1 to 4. VS-LLP produces the most accurate of the four estimates by considering the condition number of the $\arccos(\cdot)$ function [8, 10]. The approach is similar for the second component direction.

2.3. Multi-scale filterbank

Here, we consider a multi-scale approach developed by Murray and Pattichis that uses AM-FM components extracted from different scales [8, 10]. We define the scales using a collection of bandpass filters as follows: (i) LPF (lowpass filter), (ii) VL (very low frequencies), (iii) L (low frequencies), (iv) M (medium frequencies) and (v) H (high frequencies) as given in [8]. For the opacities problem, we consider eleven different combinations of scales (CoS) for extracting the dominant AM-FM estimates (see Table 1). From each combination of scales, we extract the histograms of the IA, the IF magnitude (|IF|), and the IF angle.

The motivation behind the use of scales and filterbanks is due to variability of the underlying image structures. To recognize this, we provide an example. The images that were analyzed in the preliminary study have a resolution of 300dpi. This resolution means that along 0.5mm we have 6 pixel samples. From the ILO (medical) standard, the rounded opacities labeled as p, q and r, are in the sizes up to 10mm. With the knowledge of the sizes, we can relate the lengths with the corresponding frequencies. In Table 2 we summarize these relationships. Based on the frequency ranges for each rounded opacity type used, we set up the cut-off frequencies of the bandpass filters to fit the opacities in them by each scale. Thus, we design our four-scale filter-bank such that each scale will be related with the frequency ranges described in Table 2.

Table 1. Combinations of scales used for computing the dominant AM-FM feature parameters.

CoS*	Scales used	CoS*	Scales used
1	VL, L, M, H	7	LPF, VL
2	LPF	8	VL, L
3	VL	9	L, M
4	L	10	M, H
5	M	11	H
6	LPF, VL, L, M, H		

CoS*: Combination of Scales.

Table 2. Relationship among ILO standard grades for rounded opacities, size in mm, size in pixels and range in frequency. These relationships are based on a scanning rate of 12 pixels per mm. Frequency range refers to the lowest frequency that can be used to characterize an opacity, so that we can fit at-least one wavelength inside the opacity region.

Type of rounded opacities	Range in mm	Range in pixels	Range in lowest frequency content
p	Up to 1.5	Up to 18	$[\pi/9, \pi]$
q	1.5 - 3	18 - 36	$[\pi/18, \pi/9]$
r	3 - 10	36 - 120	$[\pi/36, \pi/18]$

We use the histograms of IA and IF magnitude to create a feature vector for encoding the characteristics related with the type of opacities presented in the X-Ray image. Using histograms at different combinations of scales (see Table 1), the information extracted with AM-FM can be analyzed to find differences among different grades of the opacities. Thus, we can find if certain frequencies components that encode a feature is presented at the image.

2.4. Analysis of detection using AM-FM and Partial Least Squares

The purpose of this sub-section is to develop a predictor of disease state based on the histogram bins counts generated. The dependent variable, disease state, was coded with 0's for "normal" and 1's for the disease state. The normal images were separately compared with disease in categories 1/1 and 2/2. For each of the eleven combinations of scales (see Table 1), we use the histograms described in the previous sub-section.

We formulate the classification problem as a linear regression problem using

$$y = X\beta + \varepsilon, \quad (3)$$

where y, represents the classification: 0 for normal and 1 for abnormal, X is the extracted feature vector matrix (one row per image), β denotes the vector of regression parameters and ε represents the residuals. Using PLS, we reduce the matrix X to an order (number of factors) k such that $X \approx T_1 L_1$.

We use the ROC area of each individual CoS classification to determine the optimal number of factors for each one of the eleven Combinations of Scales in Table 1. We then select the factors from all scales, that gave the best results to form a joint feature matrix over all scales. We also select optimal factors from the joint feature matrix.

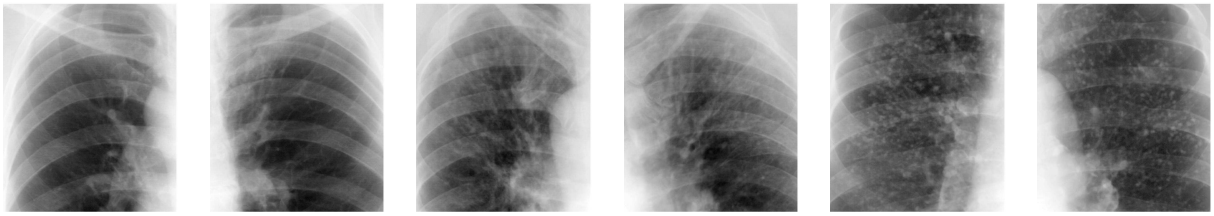

(a) (b) (c) (d) (e) (f)

Fig. 1. Example of the ROIs used from the X-Ray images (after logarithm transformation). (a)-(b) Type 0/0. (c)-(d) Type 1/1. (e)-(f) Type 2/2.

3. RESULTS

3.1. Classification using AM-FM methods

For each X-ray image (22 images in total) and for each of the 11 combinations of scales, we created a 96-bin feature vector that contains the AM-FM histograms. Each AM-FM histogram produced for each side of the lung has the information of (32-bin each): (i) the IA, (ii) the IF magnitude and (iii) the IF angle (centered around the most-frequent value). Thus, each image produces 11 different feature vectors, each one corresponding to one of the 11 different combinations from Table 1. Next, for each case from Table 1, we apply a linear regression using PLS to classify the images based on the AM-FM feature vectors.

We consider four classification problems: (i) profusion 0/0 versus 2/2, (ii) 0/0 versus 1/1, (iii) 1/1 versus 2/2 and (iv) normal versus abnormal (0/0 versus both 1/1 and 2/2 at the same time). In Table 3 we present the area under the receiver operator characteristics curve (AUC) for the training step (calibration of the PLS parameters), in terms of specificity and sensitivity, with the corresponding number of latent factor used for each combination. In general, the less number of factors we use, the more robust the classification system. To improve the robustness of our method, we create a new feature vector per image that consists of the combination of the cases that produced the best AUC individually. The goal of this procedure is to improve the classification results combining the information of all images at different scales but only in frequency ranges where the information is important. The independent AUC computed for each case together with the number of factors used give us the best cases to use. For the classification we keep the cases that produced an AUC bigger than 0.8.

3.2. Analysis of using only one combination of scales

We present an analysis of the classification when only one combination is used. From Table 3, we consider the case of classifying profusions of type 1/1 and 2/2 using combination 1 (see Table 1).

For this combination of scales, we found that PLS uses most of the information related to the IF. In Fig. 2a we show a comparison between two images 1/1 and two images 2/2 in terms of the histograms related to the |IF| and the IF angle. From Table 3, we can see that the optimum order was 2 for this case. In Fig. 2b we plot all 1/1 and 2/2 images as 2-D points where each coordinate represents a multiple of the corresponding coordinate function factor. In Fig. 2c, we show the regression parameter values (for β in (3)) for |IF|. Fig. 2d presents the same information for the IF angle.

Table 3. Area under the curve (AUC) for classification of the X-Ray images, with its corresponding number of factors, produced when by each combination independently. Best results to be used, in this case AUC > 0.8, are shown in **bold** typeface.

	Classification by categories							
	0/0 vs. 2/2		**0/0 vs. 1/1**		**1/1 vs. 2/2**		**0/0 vs. {1/1, 2/2}**	
CoS	$\mathbf{A_z}^{+}$	$\mathbf{o}^{\#}$	$\mathbf{A_z}$	**o**	$\mathbf{A_z}$	**o**	$\mathbf{A_z}$	**o**
1	**1.00**	2	**0.98**	6	**1.00**	2	**0.94**	6
2	**0.88**	4	0.78	2	**1.00**	5	0.69	2
3	**1.00**	2	0.72	13	**1.00**	2	0.79	7
4	**0.98**	2	0.72	4	**0.94**	3	0.77	2
5	**0.96**	8	**0.81**	15	**1.00**	2	**0.88**	6
6	**0.88**	4	0.78	2	**1.00**	5	0.69	2
7	**0.88**	4	0.78	2	**1.00**	5	0.69	2
8	**1.00**	2	**0.99**	6	**1.00**	2	**0.99**	6
9	**1.00**	2	**0.89**	7	**1.00**	12	**0.89**	10
10	**1.00**	2	**0.86**	4	**0.94**	5	**0.92**	7
11	**1.00**	2	**0.92**	4	**0.96**	8	**0.92**	7

A_z: Area under the ROC curve (AUC). $o^{\#}$: order or number of factors.

4. DISCUSSION

From Table 3, we note that the classification between categories 0/0 and 2/2 is the most clear. Moreover, many independent cases performed the classification using only 2 factors with an AUC equal to 1. On the other hand, the classification between types 0/0 and 1/1 is the most difficult one. From Table 3 note that none of the cases was able to produce an AUC equal to 1 independently, and the best AUC produced for this classification used at least 6 factors. However, when we use the best combinations of scales together, a perfect classification is obtained and the number of factors is 2. In terms of selecting the best cases, we kept the ones with AUC greater than 0.8.

In terms of analyzing the results by combinations of scales, we can see from Fig. 2a how the histograms are for different types of profusion are different. When we plot the locations of the images considering the two factors obtained (see Fig. 2b), the spatial separation of the types of opacities are well defined. The regression parameter uses most of the information in the IF (see Fig. 2c-d). Note in Fig. 2c the continuous positive and negative peaks. This values show us the frequencies that are subtracted for classifying the input as 'normal'.

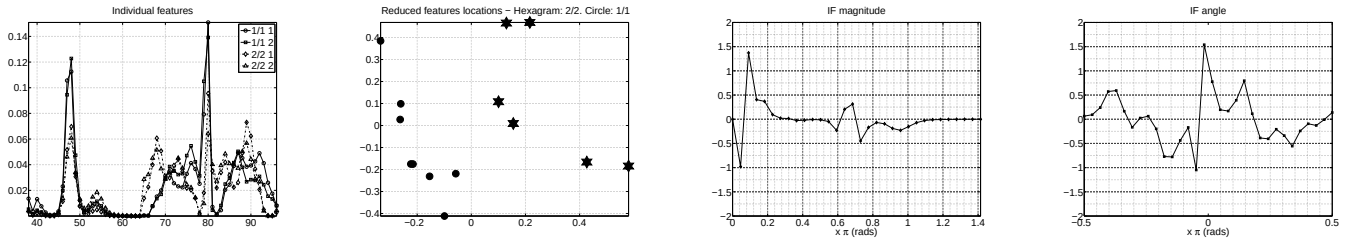

(a) (b) (c) (d)

Fig. 2. Analysis of the PLS classification using the combination of scales 1 (see Table 1). (a) Individual features for 2 images 1/1 and 2 images 2/2 in the zones of the |IF| and IF angle only. (b) Coordinate function plots for the 1/1 and 2/2 images. (c) Regression parameter for the |IF|. (d) Regression parameter for the IF angle.

5. CONCLUSIONS

We have developed a new multi-scale AM-FM classification system for classifying chest radiographs with pneumoconiosis. We have obtained excellent preliminary classification results for our limited database.

We note that the use of a single combination of scales gave excellent classification (see AUC per combination of scale in Table 3). The use of the joint combination of the best scales required only two factors for all the classification experiments. This system produces significantly better results than presented in [6, 13, 14], but in a much smaller database. In our ongoing research, the approach will be validated on a much larger database.

6. REFERENCES

[1] International Labour Office, *Guidelines for the use of ILO International Classification of Radiographs of Pneumoconioses*, Geneva, Switzerland, 1980.

[2] B. Van Ginneken, B. M. Ter Haar Romeny, and M. Viergever, "Computer-aided diagnosis in chest radiography: a survey," *IEEE Transactions on Medical Imaging*, vol. 20, no. 12, pp. 1228–1241, December 2001.

[3] H. Kondo and T. Kouda, "Computer-aided diagnosis for pneumoconiosis using neural network," in *IEEE Symposium on Computer-Based Medical Systems*, 26-27 July 2001, pp. 467–472.

[4] ——, "Detection of pneumoconiosis rounded opacities using neural network," in *Joint 9th IFSA World Congress and 20th NAFIPS International Conference*, vol. 3, 25-28 July 2001, pp. 1581–1585.

[5] M. Pattichis, T. Cacoullos, and P. Soliz, "New models for region of interest reader classification analysis in chest radiographs," *Pattern Recognition*, vol. 42, no. 6, pp. 1058 – 1066, 2009, digital Image Processing and Pattern Recognition Techniques for the Detection of Cancer.

[6] M. Pattichis, C. Pattichis, C. Christodoulou, D. James, L. Ketai, and P. Soliz, "A screening system for the assessment of opacity profusion in chest radiographs of miners with pneumoconiosis," in *IEEE Southwest Symposium on Image Analysis and Interpretation*, 7-9 April 2002, pp. 130–133.

[7] M. S. Pattichis and A. C. Bovik, "Analyzing image structure by multidimensional frequency modulation," *IEEE Transactions on Pattern Analysis and Machine Intelligence*, vol. 29, no. 5, pp. 753–766, 2007.

[8] Victor Manuel Murray Herrera, "AM-FM methods for image and video processing," Ph.D. dissertation, University of New Mexico, 2008.

[9] M. Pattichis, J. Ramachandran, M. Wilson, C. Pattichis, and P. Soliz, "Optimal scanning, display, and segmentation of the international labor organization (ILO) X-ray images set for pneumoconiosis," in *IEEE Symposium on Computer-Based Medical Systems*, 2001, pp. 511–515.

[10] V. Murray, P. Rodriguez, and M. S. Pattichis, "Multi-scale am-fm demodulation and reconstruction methods with improved accuracy," *accepted, IEEE Transactions on Image Processing*, 2009.

[11] V. Murray, M. Pattichis, and P. Soliz, "New AM-FM analysis methods for retinal image characterization," in *Asilomar Conference on Signals, Systems and Computers*, 2008.

[12] J. P. Havlicek, "AM-FM image models," Ph.D. dissertation, The University of Texas at Austin, 1996.

[13] M. Pattichis, H. Muralldharan, C. Pattichis, and P. Soliz, "New image processing models for opacity image analysis in chest radiographs," in *IEEE Southwest Symposium on Image Analysis and Interpretation*, 7-9 April 2002, pp. 260–264.

[14] P. Soliz, M. S. Pattichis, J. Ramachandran, and D. S. James, "Computer-assisted diagnosis of chest radiographs for pneumoconioses," M. Sonka and K. M. Hanson, Eds., vol. 4322, no. 1. SPIE, 2001, pp. 667–675.